

AUTOMATIC GLACIER CALVING FRONT DELINEATION ON TERRASAR-X AND SENTINEL-1 SAR IMAGERY

Lukas Krieger, Dana Floricioiu

German Aerospace Center (DLR), Remote Sensing Technology Institute (IMF)
Oberpfaffenhofen, Germany
Email: lukas.krieger@dlr.de; dana.floricioiu@dlr.de

ABSTRACT

This paper presents an approach for automatic calving front delineation of marine-terminating outlet glaciers. We utilize a Canny edge detection approach together with a shortest path optimization problem to find calving front locations (CFL) on SAR backscattering images from Sentinel-1 and TerraSAR-X. The CFLs are detected on Stripmap images acquired over Zachariae Isstrøm in Northeast Greenland where difficult conditions for CFL retrieval exist. We compare our results to CFLs that are delineated by hand and find good agreement, independent of the used sensor.

Index Terms— SAR, Calving front, Ice Sheet, Glacier, Greenland, Zachariae Isstrøm

1. INTRODUCTION

As a consequence of global warming, many observed glaciers in Greenland are losing mass. On outlet glaciers this mass loss can be partitioned in about 50% loss from surface mass balance and 50% dynamic mass loss from runoff and calving [1]. For glaciers that are grounded at the front, the calving front location (CFL) is one important parameter to calculate this dynamic mass loss component. This is the location where the glacial ice breaks off into the ocean and is no longer physically connected to the ice sheet.

Especially for tidewater glaciers, the CFL underlies strong fluctuations, both seasonally and long term. Depending on the bed topography, the front can migrate on and off stable frontal positions, where the glacier is grounded below sea level [2]. A retreat from such a stable position into an over-deepening of the fjord can lead to a detachment of the glacier from the bed followed by rapid retreat. Therefore, changes in the CFL are seen as early indicators for a glaciers' dynamic behavior [3].

In contrast to other measures for the dynamic behavior of a glacier (e.g. ice thickness, grounding line), CFLs can be directly delineated on satellite imagery. This opens up the

possibility for an automatic monitoring of a large number of outlet glaciers, given the availability of satellite data.

A variety of sensors can be utilized to detect the CFL of a glacier. However, due to insufficient solar illumination in winter at the polar and subpolar locations of many glaciers, it is difficult to track the frontal position with optical satellites throughout the whole year. Also, frequent cloud cover presents a problem for an optical approach.

The delineation of CFLs for glaciers is often treated as an edge detection problem which is a very common problem in image processing and pattern recognition. In the realm of remote sensing of the cryosphere, [4] developed an automatic approach to detect CFLs from MODIS data for outlet glaciers in East Greenland utilizing a Soebel filter. [5] published a method to map ice sheet margins from ERS-1 data and SPOT imagery.

In this paper we propose a method that is able to delineate a CFL between given start- and end points only from SAR amplitude backscattering images. In contrast to other approaches, the algorithm requires no additional data like the ice flow direction. The method is able to map the glacier front also in heavily crevassed conditions with thick ice mélange and icebergs present in front of the glacier.

2. DATA AND STUDY AREA

The CFL delineation is done on calibrated and geocoded SAR amplitude backscattering images in HH polarization. In order to delineate small cracks and crevasses, the raster images are sampled to a resolution of 10×10 m. Both a coarser or finer resolution are possible and just a trade-off between computational cost and spatial accuracy of the derived CFL.

2.1. Sentinel-1

The Sentinel-1 (S1) SAR satellite constellation has now dedicated campaigns for monitoring the Ice sheet's margins and glaciers on earth. S1 operates in Interferometric Wide Swath (IW) mode over the marine-terminating outlet glaciers of the two ice sheets. This enables us to produce updated calving front positions at least every 6 days. The ground resolution

Funded by the Deutsche Forschungsgemeinschaft (DFG, FL 848/1-1); Variations of the ice sheet geometry, ice flow and mass distribution in Northeast Greenland in the context of oceanic and atmospheric interactions.

of approximately 3×22 m is detailed enough to track small spatial features near the calving front. In this paper we use a scene from 2016-11-17 with the mission datatake id 20861 as an example for S1 imagery.

2.2. TerraSAR-X

TerraSAR-X (TSX) Stripmap mode offers a higher ground resolution than Sentinel-1 (approx. 3×3 m). Therefore, TSX allows to delineate the CFL more accurately but with a more limited spatial and temporal coverage. The focus on CFL generation with TSX should therefore lie on spatial accuracy. Additionally, the acquisitions with TSX over certain outlet glaciers reach back to 2007. Here, we utilize a Stripmap scene with the datatake id 1891217 from 2016-04-27.

2.3. Study area

Zachariae Isstrøm is located at $78.9^\circ N$, $20.5^\circ W$ in North-east Greenland. It drains a large ice mass that is called the North East Greenland Ice Stream (NEGIS) and its current flow velocity is approx. 9 m/day at its terminus. Since 2012 the glacier has been in an instable position and has retreated approximately 20 km inland [6]. Due to the high velocities, strong retreat and high latitude location, the conditions at the calving front are characterized by strong ice melange, large icebergs and a heavily crevassed terminus. As seen in Figure 1, these are conditions that complicate an accurate CFL retrieval even for the human observer.

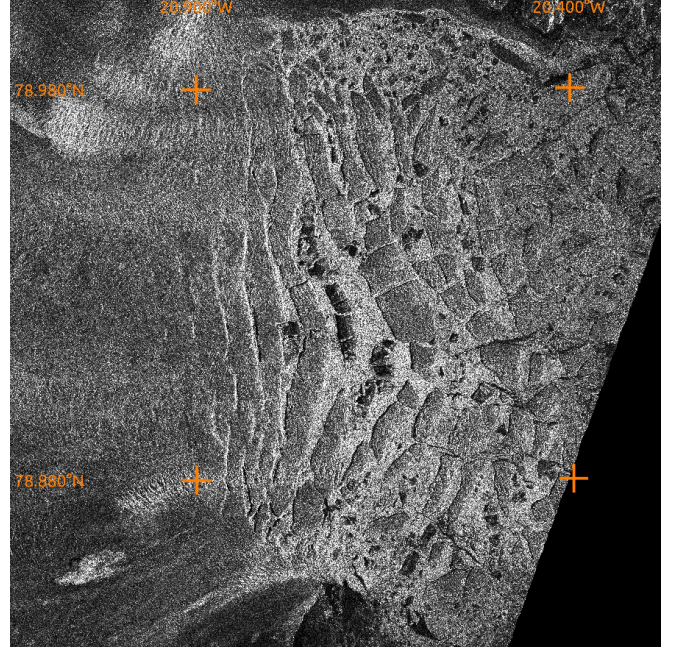


Fig. 1. The terminus of Zachariae Isstrøm observed with TSX on 2016-04-27. Multiple long crevasses, large ice bergs and heavy ice melange make it difficult to delineate a CFL even for the human observer.

We can then specify a neighborhood $S_{x,y}$ of all nodes surrounding $v_{x,y}$ as

$$S_{x,y} = \{v_{x+i,y+j} \mid v \in N, (i,j) \in \{-1,0,1\}^2 \setminus \{(0,0)\}\} \quad (3)$$

The set of edges E that defines our graph G can be constructed as

$$E = \{(v_{x,y}, v_{x',y'}) \mid v_{x,y} \in V, v_{x',y'} \in S_{x,y}\} \quad (4)$$

We describe the weights w for an edge as the pixel value of the edge end point multiplied by a weighting factor λ . Recall that I is the binary edge image resulting from the Canny Edge algorithm stated in (1).

$$w((v_{x,y}, v_{x',y'})) = I(x',y') \cdot \lambda \quad (5)$$

A path $P(v_{x_0,y_0}, v_{x_k,y_k})$ is written as $\langle v_{x_0,y_0}, \dots, v_{x_k,y_k} \rangle$ and we define its length as $|P(v_{x_0,y_0}, v_{x_k,y_k})|$ as the sum of all its edge weights. The shortest path between a given start and end node $P_s(v_s, v_e)$ is then given solving the optimization with Dijkstra's algorithm [8].

$$P_s(v_s, v_e) = \underset{v \in N}{\operatorname{argmin}} (| \langle v_s, v_{x_1,y_1}, v_{x_2,y_2}, \dots, v_e \rangle |) \quad (6)$$

The path $P_s(v_s, v_e)$ is assumed to be a good candidate for a CFL on the given backscattering amplitude image, because

3. CALVING FRONT DETECTION

To delineate the calving front automatically, we utilize the well established Canny edge detection algorithm to find edge candidates on the SAR backscattering amplitude images [7]. Let $G(x,y)$ be the magnitude of edge candidates for pixel (x,y) after the non-maximum suppression step of the Canny Edge algorithm. We define a binary image I that has values of 0 for each pixel with an edge magnitude greater than 0 and 1 otherwise.

$$I(x,y) = \begin{cases} 0 & \text{for } G(x,y) > 0 \\ 1 & \text{for } G(x,y) = 0 \end{cases} \quad (1)$$

In the following we assume that a continuous path of edge candidates ($I(x,y) = 0$) between start point v_s and end point v_e is a good indicator for the actual calving front and set up an optimization problem to find such an optimal path. We define a directed graph as $G = (V, E)$ where V is a set of nodes that reference image pixels and E contains edges that connect each image pixel to all its surrounding pixels.

Given the image dimensions $n + 1 \times m + 1$ then V is defined as

$$V = \{v_{x,y} \mid 0 < x < m, 0 < y < n\} \quad (2)$$

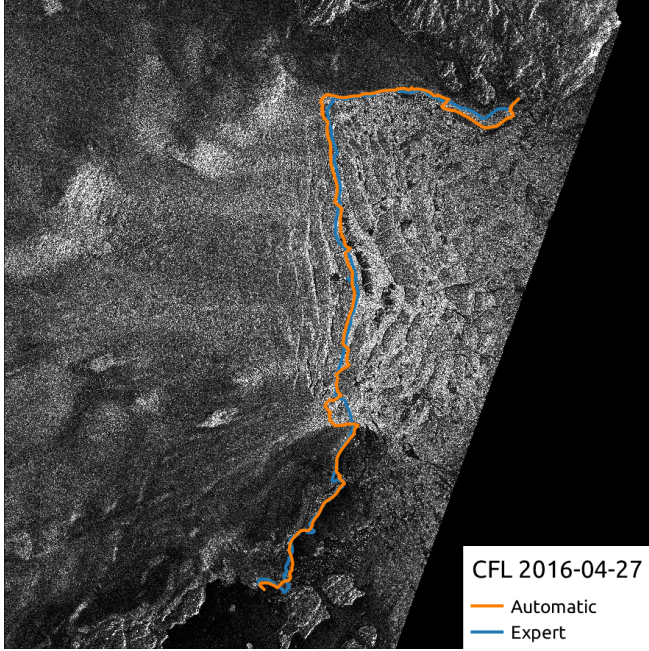


Fig. 2. The terminus of Zachariae Isstrøm observed with TSX on 2016-04-27. The automatically detected CFL is shown in orange. The blue line indicates the CFL delineated manually by an expert.

of the edge continuity between two given seed points v_s and v_e . We pick our seed points to be located at the stable coast on either side of the glacier, λ to be in the range of $[1, 100]$ and solve the optimization problem for the shortest path.

4. PRELIMINARY RESULTS AND DISCUSSION

Figure 2 and 3 show detected CFLs on Zachariae Isstrøm on amplitude backscattering images from S1 and TSX. The front locations are delineated on scenes that show varying conditions near the front with heavy ice melange, open water or ice bergs. The algorithm was tested to detect CFLs on TSX and on S1 imagery.

To judge the accuracy of the algorithmically detected calving fronts, we compare them to CFLs that are delineated by an expert with knowledge of outlet glaciers. The CFLs

Date	Sensor	λ	$\mathbb{E}(d)$ [m]
2016-11-17	Sentinel-1	50.0	246
2016-04-27	TSX	50.0	159

Table 1. The mean distance $\mathbb{E}(d)$ between the CFLs generated by an expert compared to the automatically generated CFL with processing parameter λ .

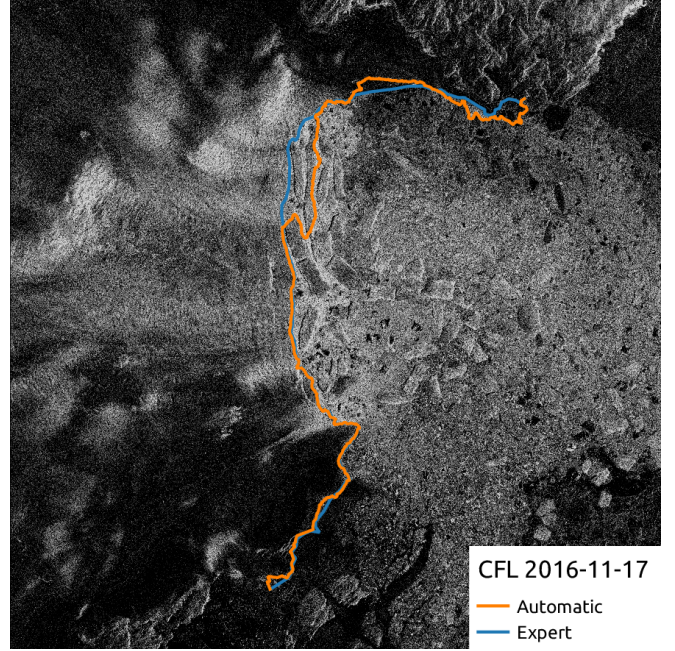


Fig. 3. The terminus of Zachariae Isstrøm observed with Sentinel-1 on 2016-11-17. The automatically detected CFL is shown in orange. The blue line indicates the CFL delineated manually by an expert.

were traced by hand on the high resolution products of the corresponding SAR amplitude image and are also shown in Figure 2 and 3. In Table 1 we present the mean difference $\mathbb{E}(d)$ between each set of CFLs (P_{expert} , $P_{\text{automatic}}$). $\mathbb{E}(d)$ is calculated with the box method, dividing the area A between both candidate lines by the average length of both delineated CFLs [9].

$$\mathbb{E}(d) = \frac{A}{\frac{|P_{\text{expert}}| + |P_{\text{automatic}}|}{2}} \quad (7)$$

In general, a better edge candidate selection also yields a more accurate CFL delineation. This step is independent of the optimization problem outlined in section 3.

5. CONCLUSION

In this paper an algorithm is presented that is able to delineate calving front locations of outlet glaciers on SAR amplitude backscattering images. CFLs are produced for Sentinel-1 and TSX data of Zachariae Isstrøm by first enhancing edges and then using a shortest path algorithm to find the best CFL candidate line. It is shown that results can even be obtained in conditions where the glacier front is crevassed and large ice bergs are present in the fjord.

6. REFERENCES

- [1] Michiel van den Broeke, Jonathan Bamber, Janneke Ettema, Eric Rignot, Ernst Schrama, Willem Jan van de Berg, Erik van Meijgaard, Isabella Velicogna, and Bert Wouters, "Partitioning recent greenland mass loss," *Science*, vol. 326, no. 5955, pp. 984–986, 2009.
- [2] Ian Joughin, Ian Howat, Richard B Alley, Goran Ekstrom, Mark Fahnestock, Twila Moon, Meredith Nettles, Martin Truffer, and Victor C Tsai, "Ice-front variation and tide-water behavior on helheim and kangerdlugssuaq glaciers, greenland," *Journal of Geophysical Research: Earth Surface*, vol. 113, no. F1, 2008.
- [3] Twila Moon and Ian Joughin, "Changes in ice front position on greenland's outlet glaciers from 1992 to 2007," *Journal of Geophysical Research: Earth Surface*, vol. 113, no. F2, 2008.
- [4] Anthony Seale, Poul Christoffersen, Ruth I Mugford, and Martin O'Leary, "Ocean forcing of the greenland ice sheet: Calving fronts and patterns of retreat identified by automatic satellite monitoring of eastern outlet glaciers," *Journal of Geophysical Research: Earth Surface*, vol. 116, no. F3, 2011.
- [5] H Liu and KC Jezek, "Automated extraction of coastline from satellite imagery by integrating canny edge detection and locally adaptive thresholding methods," *International Journal of Remote Sensing*, vol. 25, no. 5, pp. 937–958, 2004.
- [6] Jeremie Mouginot, Eric Rignot, Bernd Scheuchl, Ian Fenty, Ala Khazendar, Mathieu Morlighem, Arnaud Buzzi, and John Paden, "Fast retreat of zachariae isstrøm, northeast greenland," *Science*, vol. 350, no. 6266, pp. 1357–1361, 2015.
- [7] John Canny, "A computational approach to edge detection," *IEEE Transactions on pattern analysis and machine intelligence*, , no. 6, pp. 679–698, 1986.
- [8] Edsger W Dijkstra, "A note on two problems in connexion with graphs," *Numerische matematik*, vol. 1, no. 1, pp. 269–271, 1959.
- [9] Ian Howat and Alex Eddy, "Multi-decadal retreat of greenland's marine-terminating glaciers," *Journal of Glaciology*, vol. 57, no. 203, pp. 389–396, 2011.